Osmotic stress mechanically perturbs chemoreceptors in Escherichia coli

Osmotic stress mechanically perturbs chemoreceptors in *Escherichia coli*

Ady Vaknin and Howard C. Berg*

Department of Molecular and Cellular Biology, Harvard University, 16 Divinity Avenue, Cambridge, MA 02138; and The Rowland Institute at Harvard, 100 Edwin H. Land Boulevard, Cambridge, MA 02142

Contributed by Howard C. Berg, November 21, 2005

Two-component signaling systems play a major role in the long-term adaptation of microorganisms to changes in osmolarity, but how osmoreceptors work is not well understood. Temporal changes in solute concentration are sensed by the chemotaxis system in *Escherichia coli*, enabling these bacteria to avoid regions of high osmolarity. To study how osmolarity is detected in this system, we fused yellow fluorescent protein (YFP) to the C terminus of the serine or aspartate chemoreceptor, monitored the steady-state fluorescence polarization of YFP, and found that the polarization decreased substantially upon addition of osmotic agents. This decrease was due to an increase in fluorescence resonance energy transfer between YFP fluorophores in adjacent homodimers within trimers of dimers. Thus, changes in homodimer spacing and/or orientation appear to initiate osmotactic signaling.

bacteria | fluorescence depolarization | osmolarity | signal transduction | yellow fluorescent protein

The bacterium *Escherichia coli* has several membrane-spanning chemoreceptor species; the two most abundant sense serine (Tsr) or aspartate (Tar). These receptors form homodimers (1) that in turn assemble to form what are thought to be trimers of dimers composed of the same or different homodimer species (2–5). The receptors control the activity of an associated cytoplasmic kinase, CheA, that donates phosphate to a response regulator, CheY, that when phosphorylated binds to the base of the flagellar motors, affecting their direction of rotation and, thus, controlling the motile behavior of the bacterium. The lifetime of phosphorylated CheY is shortened by the action of a dedicated phosphatase, CheZ. Inspired by the early work of J. Massart (6), Adler and coworkers (7, 8) showed that the chemotaxis system in *E. coli* can sense changes in general solute concentration. In response to mild up-shifts in osmolarity (200–300 mOsm), the rotational bias of the flagellar motors shifts toward clockwise, enhancing tumbling, and thereby enabling cells to avoid regions of high osmolarity. This behavior can be mediated by any one of the chemoreceptor species, but how the receptors do this was not determined. For recent studies of the mechanisms underlying osmodetection in other two-component systems, see refs. 9–13. By constructing fluorescence protein fusions to chemoreceptors and monitoring changes in their fluorescence polarization, we show that osmotic stress compresses receptor trimers.

Results

To study the effect of osmotic stress on the chemoreceptors, we fused yellow fluorescent protein (YFP) to the C terminus of Tsr or Tar (see *Methods*). Some of the properties of these receptor fusions are shown in Fig. 1. YFP is small compared to Tar or Tsr (Fig. 1*a*). When expressed in a receptor-deletion background (UU1250), both Tsr-YFP and Tar-YFP gave rise to normal motor bias, measured by tethering cells to a microscope slide, and they responded normally to addition of serine or aspartate; however, they did not form chemotactic rings on soft-agar bacto-tryptone plates (data not shown). The failure of these cells to support chemotaxis is expected, given that YFP is likely to block the methyltransferase/methylesterase (CheR/CheB) binding site at the receptor C terminus and, thus, to inhibit adaptation (14, 15). Changes in kinase activity were measured more quantitatively by expressing Tsr-YFP in *tsr tar tap trg cheR cheB cheY cheZ* cells together with CheY-YFP and CheZ-CFP and measuring the association between YFP and cyan fluorescent protein (CFP) by using fluorescence resonance energy transfer (FRET) (Fig. 1*b* and see *Methods*). The resultant dose–response curve is similar to those obtained with wild-type Tsr receptors (16). Finally, fluorescence images of Tsr-YFP expressed in *tsr tar tap cheR cheB cheY cheZ* cells showed that receptor fusions were clearly able to form tight clusters (Fig. 1*c*). More receptors are seen along the sides of the cells in these images than are apparent when receptors are labeled by cytoplasmic proteins, such as CheR-YFP (17), presumably because the label is localized entirely to the membrane. We conclude that, apart from adaptation, the receptor-YFP fusions are functional.

The effect of osmotic stress was measured by fluorescence polarization in a microscope-based system. Cells immobilized on a cover slip and mounted in a flow cell were excited at 510 nm with linearly polarized light and the parallel (I_{par}) and perpendicular (I_{per}) components of the emitted fluorescence were measured (see *Methods*). The steady-state polarization of the emitted fluorescence is represented here by the fluorescence anisotropy, r, defined as $(I_{par} - I_{per})/(I_{par} + 2I_{per})$, where I_{per} has been corrected for imperfections of the optical system (18), in our case by a factor of 0.99. Typical anisotropy traces are shown in Fig. 2 for cells expressing Tsr-YFP (red symbols) or free YFP (green symbols). During these experiments, various solutes were added or removed, as indicated. In the case of free YFP, the anisotropy level, $r \approx 0.32$, is close to the value found previously in studies using spectrofluorometers (19). In the case of Tsr-YFP, however, the basal anisotropy level was consistently lower. Because tethering to the receptor cannot enhance the rotational diffusion of YFP, such reduced anisotropy is likely the result of homo-FRET between YFP fluorophores (19). The anisotropy of the fluorescence of Tsr-YFP decreased substantially upon addition of 50 mM sodium chloride, 100 mM sucrose, or 100 mM dextran (Fig. 2*a*). Similar responses (data not shown) were obtained upon addition of stachyose (100 mM) or poly(L)-glutamate (molecular weight 17,400; 2.5% wt/vol). On the other hand, 300 mM glycerol or 300 mM ethanol, which rapidly enter the cytoplasm (20, 21), failed to generate a response (Fig. 2*a*). The nature of the solutes that were able to generate a response implicates osmolarity as the essential stimulus. The corresponding changes in the anisotropy of free YFP upon addition of those solutes were relatively small and of opposite sign, indicating that the responses measured with Tsr-YFP did not occur as a result of nonspecific effects of osmolarity on the YFP fluorophore.

Conflict of interest statement: No conflicts declared.

Abbreviations: YFP, yellow fluorescent protein; CFP, cyan fluorescent protein; IPTG, isopropyl β-D-thiogalactopyranoside.

*To whom correspondence should be addressed. E-mail: hberg@mcb.harvard.edu.

www.pnas.org/cgi/doi/10.1073/pnas.0510047103

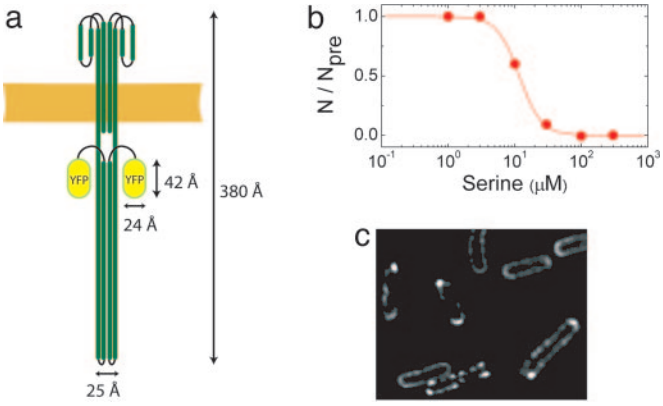

Fig. 1. Properties of receptor-YFP fusions. (*a*) A scale drawing of a single homodimer inferred from the known structures of Tsr (2) and GFP (35). (*b*) A dose–response curve for serine measured with Tsr-YFP (pAV36) coexpressed with CheZ-CFP and CheY-YFP (pVS88) in *tsr tar tap trg cheR cheB cheY cheZ* cells (strain VS164). The kinase activity (represented by N/N_{pre}, the number of CheZ-CheY pairs normalized by the prestimulus value) was deduced by measuring FRET between CFP and YFP (see *Methods*). (*c*) Representative fluorescence images of Tsr-YFP (pAV29) in *tsr tar tap cheR cheB cheY cheZ* cells (VS170).

To verify the role of receptor assembly, we measured the polarization response of YFP fused to receptor mutants that are known to be defective in trimer formation (Fig. 3). $Tar_{1–279}$ is a truncated version of Tar. It still spans the membrane but is missing most of the cytoplasmic domain, including the entire trimer contact region. Indeed, the anisotropy of the fluorescence from $Tar_{1–279}$-YFP (green symbols) did not decrease upon osmotic up-shift but even slightly increased, as seen with free YFP. Tsr^{I337P}-YFP carries a point mutation in the trimer contact region of Tsr known to cause a defect in trimer formation (3, 4). Accordingly, its anisotropy response (Fig. 3, blue symbols) was considerably smaller than that found with wild-type Tsr-YFP (Fig. 3, red symbols). In addition, as with free YFP (Fig. 2), the fluorescence from both mutants was consistently more anisotropic than that from wild-type receptors, indicating that substantially less homo-FRET occurs in the mutants. These results clearly show that the polarization response relies upon receptor assembly and, in particular, upon trimer formation. Note also that the fluorescence from the mutants was less anisotropic than that from free YFP, presumably because of homo-FRET between different YFPs on the same homodimer.

To verify the role of homo-FRET, we performed *in vivo* mixing experiments. We coexpressed a constant level of labeled receptors, Tar-YFP or Tsr-YFP, with increasing amounts of nonlabeled ones, Tar or Tsr. Assembly of the nonlabeled receptors together with the labeled ones should increase the average distance between the YFP proteins in the receptor assemblies, leading to a reduced FRET efficiency. Anisotropy traces recorded from Tsr-YFP coexpressed with low (filled symbols) or high (open symbols) levels of nonlabeled Tar are shown in Fig. 4*a*. Coexpression of nonlabeled Tar increased the basal anisotropy level and diminished the response to addition of sucrose, a behavior similar to that seen when receptor assemblies were disrupted in receptor mutants. The response amplitudes to addition of sucrose are plotted in Fig. 4*b* as a function of the levels of induction of the nonlabeled receptors for various receptor combinations. The anisotropy response progressively diminished as the expression of nonlabeled receptors increased (Fig. 4*b*, green and red symbols) but less so with a Tsr mutant (I377P) defective in trimer formation (Fig. 4*b*, blue symbols). These results indicate that the polarization response does indeed rely on interactions between the YFP molecules and thus strongly implicates FRET as the primary cause.

The simplest receptor assembly is the homodimer (Fig. 1*a*), comprising two receptors of the same kind; dimers containing receptors of different kinds are not observed (1). If the polarization response were dominated by modulation of FRET between YFP molecules within a homodimer, nonlabeled Tsr would not affect the response of Tar-YFP, and nonlabeled Tar would not affect the response of Tsr-YFP. However, Tar and Tsr were equally effective

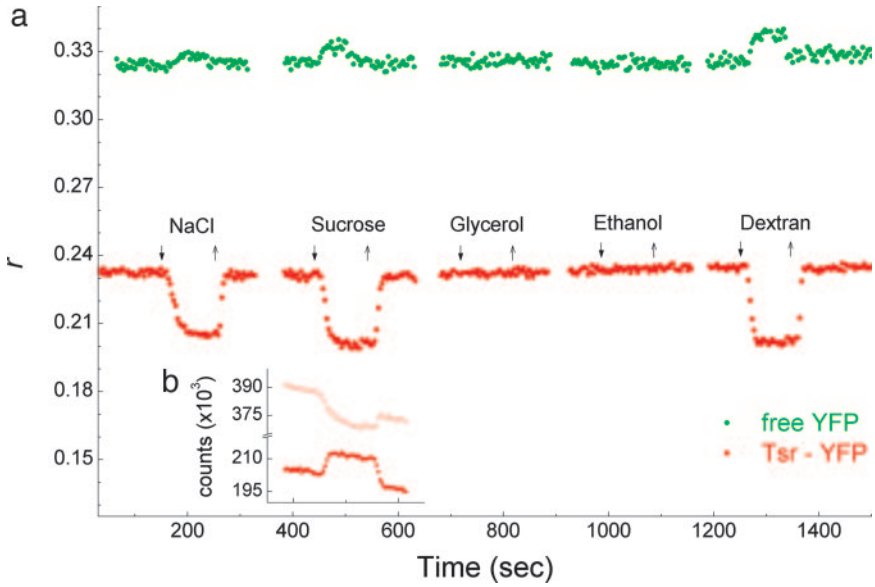

Fig. 2. Response of the fluorescence anisotropy of Tsr-YFP to osmotic stress. (*a*) The steady-state anisotropy, *r*, of the fluorescence emitted from a population of ≈100 cells was recorded, whereas various solutes were added (↓) or removed (↑), as indicated. Traces are shown for *tsr tar tap cheR cheB cheY cheZ* cells (strain VS170) expressing Tsr-YFP (pAV29; red symbols) or free YFP (pAV41; green symbols). Solute concentrations were 50 mM NaCl, 100 mM sucrose, 300 mM glycerol, 300 mM ethanol, and 100 mM dextran (molecular weight 1,500). (*b*) The raw fluorescence intensity (in photon counts, integrated over 3 sec) in the parallel (open symbols) and perpendicular (filled symbols) channels recorded from Tsr-YFP during the sucrose stimulus.

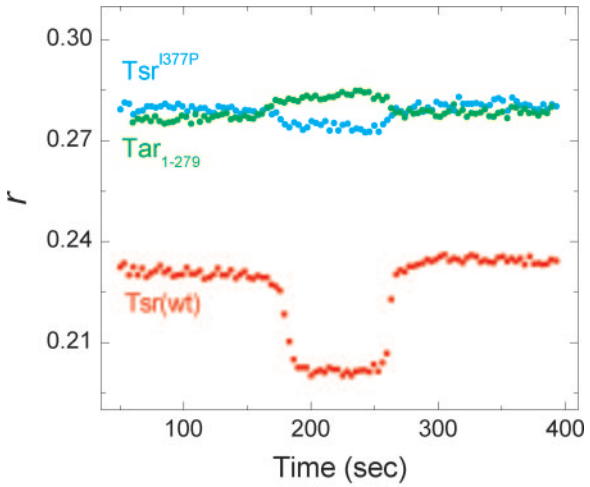

Fig. 3. Fluorescence anisotropy responses of various receptor mutants. The steady-state fluorescence anisotropy, *r*, was recorded, as in Fig. 2, while sucrose (100 mM) was added and then removed: the wild type Tsr-YFP (pAV29) in red symbols, and the mutants $Tar_{1–279}$-YFP (pAV28) and Tsr^{I377P}-YFP (pAV30) in green and blue symbols, respectively. Fusions were expressed in *tsr tar tap trg aer* cells (strain UU1250).

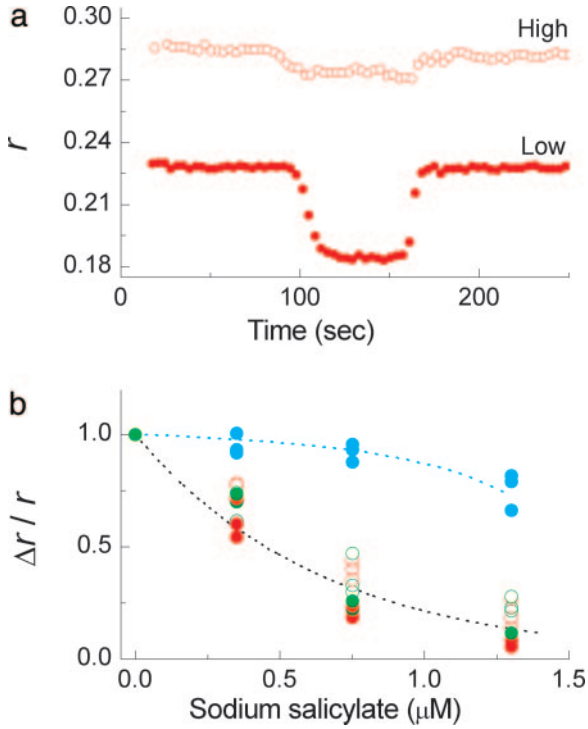

Fig. 4. Mixing experiments: coexpression of a fixed amount of labeled receptors with increasing amounts of nonlabeled receptors. (*a*) Anisotropy responses to addition of 200 mM sucrose recorded from *tsr tar tap cheR cheB cheY cheZ* cells (strain VS170) coexpressing a fixed amount of Tsr-YFP (pAV29) together with a low level of nonlabeled Tar (pLC113), induced by 0 μM sodium salicylate (filled symbols), or with a high level of nonlabeled Tar, induced by 1.3 μM sodium salicylate (open symbols). (*b*) The relative response amplitude, $\Delta r/r$, obtained from cells coexpressing Tsr-YFP (pAV29; open symbols) or Tar-YFP (pAV32; filled symbols) together with Tsr (pPA114; green symbols), Tar (pLC113; red symbols), or Tsr^{I377P} (pCS12; blue symbols) expressed at different levels relative to the labeled receptors. Data were normalized by the response at 0 μM sodium salicylate. Lines are a guide to the eye. The abscissa is labeled by the concentration of sodium salicylate used to induce the nonlabeled receptors (0, 0.35, 0.75, and 1.3 μM). The corresponding expression levels were quantified by immunoblotting (see *Methods*) and were found to be similar for the three nonlabeled receptors. The corresponding fraction of labeled receptors (labeled receptors/total receptors) was estimated for the Tar-YFP fusion to be ≈0.7, 0.25, 0.08, and 0.05, respectively. The shift of the Tsr-YFP data (open symbols) relative to that of the Tar-YFP data (filled symbols) is consistent with the higher level of expression of Tsr-YFP.

in diminishing the responses of Tar-YFP or Tsr-YFP, as shown in Fig. 4*b* (red vs. green symbols). On the other hand, the nonlabeled Tsr^{I377P}, which is defective in trimer formation, had little effect on the response from Tar-YFP (Fig. 4*b*, blue symbols). Evidently, the nonlabeled receptors that strongly affect the polarization do so via their ability to form mixed trimers with the labeled receptors. These results further support the conclusion that interdimer interactions dominate the response.

Fig. 5 shows the downstream effect of osmolarity on the level of receptor kinase activity. *cheY cheZ* cells expressing CheY-YFP and CheZ-CFP were fixed in a flow cell, and the changes in the level of FRET were detected by monitoring the ratio of the yellow to cyan fluorescence, Y_F/C_F (see *Methods*). Upon addition of sucrose (100 mM), the kinase activity increased and then adapted back to its basal level. Upon removal of sucrose, the kinase activity decreased and again adapted back to its basal level. These responses are consistent with the observation that chemotactic cells are repelled by high osmolarity (7).

Discussion

As shown by Adler and coworkers (7, 8) and reiterated in Fig. 5, osmotic agents act as repellents. Upon their addition, receptor kinase activity is enhanced, and then cells adapt. We have found that addition of osmotic agents decreases the anisotropy of the emission of YFP fused to the C terminus of wild-type receptors (Fig. 2, red symbols). On the other hand, addition of the same agents slightly increases the anisotropy of the fluorescence emitted from free YFP (Fig. 2; green symbols) or from YFP fused to receptor fragments that still span the membrane, $Tar_{1–279}$-YFP (Fig. 3, green symbols). The latter results rule out the possibility that the response seen with wild-type receptors is due to some nonspecific effect of osmotic up-shift on the YFP fluorophore. The response seen with free YFP might result from an increase in molecular crowding after efflux of water from the cytoplasm. The mutation analyses (Fig. 3) and the *in vivo* mixing experiments (Fig. 4) strongly suggest that the polarization responses of wild-type receptor fusions occur via modulation of FRET between YFP molecules in adjacent homodimers resulting from mechanical perturbations in the structure of trimers of dimers.

Mechanical responses of the chemoreceptors to osmotic stress most likely occur via interaction of the receptors with the cytoplasmic membrane. Addition of osmotic agents causes an efflux of water, which reduces the cells' turgor pressure, leading to reduced lateral membrane tension and increased membrane thickness. These changes would affect hydrophobic interactions between the membrane and transmembrane receptor domains and thus could alter the relative orientation and/or spacing of these domains and perturb trimer structure. Similar effects are thought to trigger the response of other mechanosensitive elements, such as gramicidin and mechanosensitive channels (22–25). The simplest interpretation of our results is that osmotic stress compresses receptor trimers: as the transmembrane domains change their orientation, the arms of a trimer move closer together, and the exchange of fluorescence energy between YFP molecules within the trimer is enhanced. To check the plausibility of such a scenario, we estimated the minimum amount of dimer tilting that would be needed to produce the observed change in anisotropy. This estimate relies on the following assumptions. All homodimers are assembled into trimers, and they all undergo similar transformation upon osmotic up-shift. The observed response is entirely attributable to modulation of

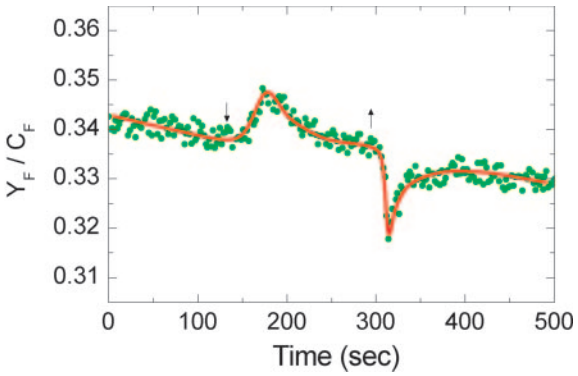

Fig. 5. Changes in receptor kinase activity after an osmotic stimulus. *cheY cheZ* cells (strain VS104) expressing CheY-YFP (pVS18) and CheZ-CFP (pVS54) were excited with 440 nm light, and the yellow (Y_F) and cyan (C_F) fluorescences were recorded from ≈100 cells. The ratio Y_F/C_F is shown as a function of time (see *Methods*). Sucrose (100 mM) was added (↓) and then removed (↑), as indicated by the arrows.

FRET between YFP molecules that occur because of changes in their separation. No higher-order FRET transitions from the acceptor back to the donor occur. The motion of YFP is unhindered, so given a high enough FRET efficiency, the anisotropy can approach zero. Under these assumptions, the relation between the steady-state anisotropy and the distance between the fluorophores is given by $r/r_0 = f/(1 + f)$, where $f = (R/R_0)^6$, r_0 is the anisotropy in the absence of FRET, R is distance between fluorophores, and R_0 is the distance over which the FRET efficiency is reduced to 50% (26). Solving for R we get $R = R_0 \cdot (r_0/r - 1)^{-1/6}$. Taking r_0 to be 0.285, the polarization in the absence of homo-FRET promoted by trimer formation (Fig. 3), we find that the anisotropy will change from 0.23 to 0.20 (Fig. 2) if R decreases by ≈10%. The length of the cytoplasmic part of a receptor is ≈260 Å (2); thus, if the spacing between transmembrane domains of different dimers within a trimer is ≈100 Å (2, 27), the angle between dimers (connected at their cytoplasmic tips) would be ≈20°. Therefore, a 10% change in the distance between the transmembrane domains would correspond to an ≈2° change in the relative angle between dimers. Clearly, such a small change in orientation is plausible.

Evidently, receptor trimers are perturbed mechanically by osmotic stress, presumably via interactions with the membrane. Somehow, these perturbations enhance kinase activity. One would expect perturbations of the opposite sign to occur upon addition of chemoattractants.

Methods

Bacterial Strains. All strains were derivatives of *E. coli* K12 strain RP437. Strains VS104 (*cheY cheZ*), VS164 (*tsr tar tap trg cheR cheB cheY cheZ*), and VS170 (*tsr tar tap cheR cheB cheY cheZ*) were a gift from Victor Sourjik (University of Heidelberg, Heidelberg), and strain UU1250 (*tsr tar tap trg aer*) was a gift from Sandy Parkinson (University of Utah, Salt Lake City). Cells were grown overnight in 5 ml of bacto-tryptone (10 g/liter; Difco), diluted 100-fold in 10 ml of bacto-tryptone supplemented with the appropriate antibiotics and inducers, and allowed to grow to OD_{600} ≈0.45. No extra salt (5 g/liter NaCl) was added to the growth medium, to avoid adaptation to additional osmotic stress, although osmotic responses were observed even when it was included. Cells were washed and resuspended in motility medium (buffer: 10 mM potassium phosphate/0.1 mM EDTA/1 μM methionine/10 mM lactic acid, pH 7).

Plasmids. An *A206K* mutation was introduced in *eyfp* (Clontech) to eliminate the self-association of its gene product (28). This variant of YFP was used throughout, except in pVS18 and pVS88 (see below). For simplicity, we refer to the gene as yfp^{A206K} and its product as YFP. Vectors carrying *tar* (pLC113), *tsr* (pPA114), and tsr^{I337P} (pCS12) under control of a sodium salicylate-inducible promoter were a gift from Sandy Parkinson (3, 29). *tsr* and tsr^{I337P} were amplified from these plasmids by using PCR (starting at the EcoRI site), fused to yfp^{A206K} via a GlySer$(Gly)_4$Val linker, and cloned in pTrc99A (30) to form plasmids pAV29 carrying *tsr*-yfp^{A206K} and pAV30 carrying tsr^{I337P}-yfp^{A206K}. These plasmids conferred ampicillin resistance and were inducible by isopropyl β-D-thiogalactopyranoside (IPTG); ≈6 μM IPTG was used. Plasmid pAV32 carrying *tar*-yfp^{A206K} was constructed by replacing *tsr* in pAV29 with *tar* from pDK56 (a gift from Victor Sourjik), using NcoI and BamHI sites. This plasmid was induced with ≈12 μM IPTG. Expression levels of Tar-YFP and Tsr-YFP were estimated on the basis of relative fluorescence and immunoblotting to be ≈3-fold and 6-fold times larger, respectively, than native levels in wild-type strain RP437. Plasmid pAV28 carrying tar_{1-279}-yfp^{A206K} also was cloned in pTrc99A: *tar* was cut at its endogenous KpnI site and fused to yfp^{A206K} via a $(Gly)_5$Val linker. yfp^{A206K} was cloned in pTrc99A vector to form plasmid pAV41 and was induced with 20 μM IPTG. Plasmid pAV36 carrying *tsr*-yfp^{A206K} under the control of arabinose-inducible promoter was constructed by moving *tsr*-yfp^{A206K} from pAV29 to vector pBAD33 (31), conferring chloramphenicol resistance. This plasmid was induced with 0.01% (wt/vol) arabinose. Plasmids pVS88 (carrying *cheZ-cfp* and *cheY-yfp*), pVS18 (carrying *cheY-yfp*), and pVS54 (carrying *cheZ-cfp*), were a gift from Victor Sourjik (16, 32). pVS88 and pVS18 were induced with 50 μM IPTG, and pVS54 was induced with 0.01% (wt/vol) arabinose.

Immunoblotting. Cells were grown as described above, disrupted by either sonication or addition of trichloroacetic acid (33), boiled for 5 min in SDS loading buffer, and applied (10 μl per lane) to a 7.5% Tris·HCl precast gel (Bio-Rad). Proteins were blotted for 20 min at 10 V in a semidry blotter (Bio-Rad) and detected with an antibody raised against the cytoplasmic domain of Tsr (a gift from Sandy Parkinson); this antibody recognizes Tar as well as Tsr. Relative levels of expression were estimated by comparing the intensities of corresponding bands at various dilutions.

Fluorescence Polarization Measurements. A Nikon Optiphot microscope equipped with a ×40 plan Fluor 0.65 numerical aperture objective was used. A 75-W xenon lamp served as a light source. A Glan-Thompson polarizer (for prepolarization; ThorLabs, Newton, NJ) and a linear glass polarizer (extinction ratio 10,000:1; Edmund Optics, Barrington, NJ) were used to polarize the excitation beam, which then passed through an HQ510/10x excitation filter and was reflected by a Q520LP dichroic mirror (Chroma Technology, Brattleboro, VT) to excite the YFP fluorophore. The emitted light passed through the dichroic mirror, was filtered by an HQ545/30m emission filter, and then was split with a polarizing beamsplitter cube (extinction ratio >500; New Focus, San Jose, CA). The beams passing through the polarizers and filters were all collimated, i.e., nonconverging. The two polarization channels were monitored with photon counters (H7421–40; Hamamatsu, Bridgewater, NJ) connected to a PCI NI6251 data-acquisition card controlled by LABVIEW (National Instruments, Austin, TX). The light intensity recorded from cells that did not express YFP was ≈1% of the intensity recorded during the measurements presented here. Validation of the absolute fluorescence anisotropy was done by adjusting the anisotropy recorded from a 0.3 μM aqueous solution of

fluorescein to zero (34). Experiments were done at room temperature (22°C).

Fluorescence Imaging. Images shown in Fig. 1*c* were obtained by using a DeltaVision deconvolution system (Applied Precision, Issaquah, WA) based on an Olympus IX70 inverted microscope.

Kinase Activity Measurements Using FRET. At steady state, the kinase activity is proportional to the level of association between phosphorylated CheY and CheZ, which can be measured by FRET and represented by the ratio between the yellow (Y_F) and the cyan (C_F) emissions, as described earlier (32). Cells expressing CheY-YFP and CheZ-CFP were excited at 440 nm, and the cyan (465–505 nm) and yellow (520–550 nm) emissions were monitored.

We thank V. Sourjik and J. S. Parkinson for strains, plasmids, and reagents, T. S. Shimizu for helpful conversations, and R. B. Bourret for critical reading of the manuscript. This work was supported by National Institutes of Health Grant AI016478.

1. Milligan, D. L. & Koshland, D. E., Jr. (1988) *J. Biol. Chem.* **263,** 6268–6275.
2. Kim, K. K., Yokota, H. & Kim, S.-H. (1999) *Nature* **400,** 787–792.
3. Ames, P., Studdert, C. A., Reiser, R. H. & Parkinson, J. S. (2002) *Proc. Natl. Acad. Sci. USA* **99,** 7060–7065.
4. Studdert, C. A. & Parkinson, J. S. (2004) *Proc. Natl. Acad. Sci. USA* **101,** 2117–2122.
5. Parkinson, J. S., Ames, P. & Studdert, C. A. (2005) *Curr. Opin. Microbiol.* **8,** 116–121.
6. Massart, J. (1889) *Arch. Biol. (Liege)* **9,** 515–570.
7. Adler, J., Li, C., Boileau, A. J., Qi, Y. & Kung, C. (1988) *Cold Spring Harbor Symp. Quant. Biol.* **53,** 19–22.
8. Li, C. & Adler, J. (1993) *J. Bacteriol.* **175,** 2564–2567.
9. Heermann, R. & Jung, K. (2004) *Curr. Opin. Microbiol.* **7,** 168–174.
10. Hohmann, S. (2002) *Microbiol. Mol. Biol. Rev.* **66,** 300–372.
11. Poolman, B., Blount, P., Folgering, J. H. A., Friesen, R. H. E., Moe, P. C. & van der Heide, T. (2002) *Mol. Microbiol.* **44,** 889–902.
12. Westfall, P. J., Ballon, D. R. & Thorner, J. (2004) *Science* **306,** 1511–1512.
13. Wood, J. M. (1999) *Microbiol. Mol. Biol. Rev.* **63,** 230–262.
14. Barnakov, A. N., Barnakova, L. A. & Hazelbauer, G. L. (1999) *Proc. Natl. Acad. Sci. USA* **96,** 10667–10672.
15. Wu, J., Li, J., Li, G., Long, D. G. & Weis, R. M. (1996) *Biochemistry* **35,** 4984–4993.
16. Sourjik, V. & Berg, H. C. (2004) *Nature* **428,** 437–441.
17. Sourjik, V. (2004) *Trends Microbiol.* **12,** 569–576.
18. Lakowicz, J. R. (1999) *Principles of Fluorescence Spectroscopy* (Kluwer Academic/Plenum, New York), 2nd Ed.
19. Lidke, D. S., Nagy, P., Barisas, B. G., Heintzmann, R., Post, J. N., Lidke, K. A., Clayton, A. H. A., Arndt-Jovin, D. J. & Jovin, T. M. (2003) *Biochem. Soc. Trans.* **31,** 1020–1027.
20. Stock, J. B., Rauch, B. & Roseman, S. (1977) *J. Biol. Chem.* **252,** 7850–7861.
21. Heller, K. B., Lin, E. C. C. & Wilson, T. H. (1980) *J. Bacteriol.* **144,** 274–278.
22. Goulian, M., Mesquita, O. N., Fygenson, D. K., Nielsen, C., Andersen, O. S. & Libchaber, A. (1998) *Biophys. J.* **74,** 328–337.
23. Hamill, O. P. & Martinac, B. (2001) *Physiol. Rev.* **81,** 685–740.
24. Kung, C. (2005) *Nature* **436,** 647–654.
25. Poolman, B., Spitzer, J. J. & Wood, J. M. (2004) *Biochim. Biophys. Acta* **1666,** 88–104.
26. Krishnan, R. V., Varma, R. & Mayor, S. (2001) *J. Fluorescence* **11,** 211–226.
27. Shimizu, T. S., Le Novere, N., Levin, M. D., Beavil, A. J., Sutton, B. J. & Bray, D. (2000) *Nat. Cell Biol.* **2,** 792–796.
28. Zacharias, D. A., Violin, J. D., Newton, A. C. & Tsien, R. Y. (2002) *Science* **296,** 913–916.
29. Studdert, C. A. & Parkinson, J. S. (2005) *Proc. Natl. Acad. Sci. USA* **102,** 15623–15628.
30. Amann, E., Ochs, B. & Abel, K. J. (1988) *Gene* **69,** 301–315.
31. Guzman, L. M., Belin, D., Carson, M. J. & Beckwith, J. (1995) *J. Bacteriol.* **177,** 4121–4130.
32. Sourjik, V. & Berg, H. C. (2002) *Proc. Natl. Acad. Sci. USA* **99,** 123–127.
33. Li, M. & Hazelbauer, G. L. (2004) *J. Bacteriol.* **186,** 3687–3694.
34. Clayton, A. H. A., Hanley, Q. S., Arndt-Jovin, D. J., Subramaniam, V. & Jovin, T. M. (2002) *Biophys. J.* **83,** 1631–1649.
35. Ormo, M., Cubitt, A. B., Kallio, K., Gross, L. A., Tsien, R. Y. & Remington, S. J. (1996) *Science* **273,** 1392–1395.